Production of electronically excited N_2^+ ions by electron impact on N_2 molecules

John T. Fons, James S. Allen, R. Scott Schappe, and Chun C. Lin

Department of Physics, University of Wisconsin, Madison, Wisconsin 53706

Measurements of the optical emission cross sections for the N_2^+ $D^2\Pi_g \to A\,^2\Pi_u$ emission bands produced by electron impact on N_2 are reported. From these optical data, estimates of the apparent cross sections for the electron-impact production of N_2^+ ($D\,^2\Pi_g$) in the vibrational states $v = 4$, 7, and 9 are obtained. Combining these data with similar cross sections for the $A\,^2\Pi_u \to X\,^2\Sigma_g^+$ and $B\,^2\Sigma_u^+ \to X\,^2\Sigma_g^+$ bands and with ionization cross sections of N_2 enables us to analyze the systematics of the cross sections for producing N_2^+ in the $X\,^2\Sigma_g^+$, $A\,^2\Pi_u$, $B\,^2\Sigma_u^+$, and $D\,^2\Pi_g$ states. Two different kinds of excitation behaviors are found and are discussed in reference to the electronic structure of the N_2^+ ion.

PACS number(s): 34.80.Gs

I. INTRODUCTION

Production of electronically excited N_2^+ by electron bombardment on N_2 molecules has been a subject of continual interest. The $B\,^2\Sigma_u^+ \to X\,^2\Sigma_g^+$ emission (first negative band system) of N_2^+ is one of the most prominent band systems of nitrogen. The electron-impact excitation for this band system is of considerable importance in atmospheric research. The Meinel band system ($A\,^2\Pi_u \to X\,^2\Sigma_g^+$) of N_2^+ is often seen in the aurora. Cross sections for exciting the first negative band system and the Meinel band system by electron collision with N_2 molecules have been previously measured [1–8] and apparent cross sections for the vibrational levels of the first

FIG. 1. Energy curves for the ground electronic states of N_2 and N_2^+ and for the first three excited electronic states of N_2^+.

two electronically excited states of N_2^+, $A\,^2\Pi_u$ and $B\,^2\Sigma_u^+$, have been determined. Experiments on the excitation of the $C\,^2\Sigma_u^+$ state of N_2^+ by electron impact on N_2 have also been reported [9]. The analysis of the $C\,^2\Sigma_u^+ \to X\,^2\Sigma_g^+$ emission bands (second negative system), however, is complicated by the predissociation of the $C\,^2\Sigma_u^+$ state.

The next electronically excited state above the $B\,^2\Sigma_u^+$ state is the $D\,^2\Pi_g$ state [10]. Figure 1 shows the energy curves [10] for the ground electronic states of N_2 and N_2^+ and for the first three excited electronic states of N_2^+. The $D \to A$ emission (the Janin-d'Incan band system) has been observed in nitrogen discharges [10]. In this paper we report measurements of optical emission cross sections of vibrational bands of the $D\,^2\Pi_g \to A\,^2\Pi_u$ transitions. By combining the cross-section data for the $A\,^2\Pi_u$, $B\,^2\Sigma_u^+$, and $D\,^2\Pi_g$ states of N_2^+ with the total ionization cross-section data for production of N_2^+ [11,12], we study the systematics of the processes that lead to the production N_2^+ in the various electronic states and discuss them in terms of the electronic structure of the N_2^+ ion.

II. EXPERIMENT

The principal elements of the experimental apparatus used to measure the optical emission cross sections of the N_2^+ $D\,^2\Pi_g \to A\,^2\Pi_u$ bands are described in Refs. [13] and [14], thus only a brief outline of the experimental procedure and the modification of the detection technique is presented here. An electron gun produces a collimated, monoenergetic electron beam inside a collision chamber filled with N_2 gas. The N_2^+ $D\,^2\Pi_g \to A\,^2\Pi_u$ emission from a short segment of the electron beam is observed perpendicular to the electron-beam axis and a limiting stop S after the mirror $M1$ defines the solid angle of observation as shown in Fig. 2. The mirror $M2$ images the electron beam onto the monochromator entrance slit and the dispersed radiation is detected by a photomultiplier tube (PMT) at the monochromator exit slit. The output of the PMT is recorded as a function of wavelength and the optical emission cross section of a
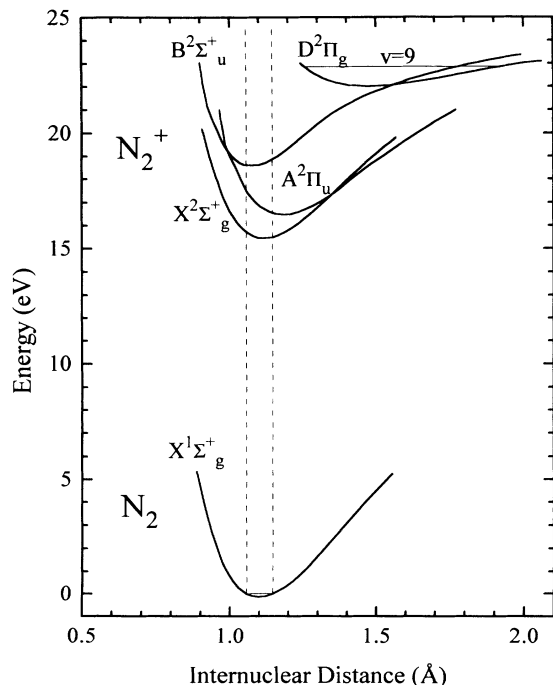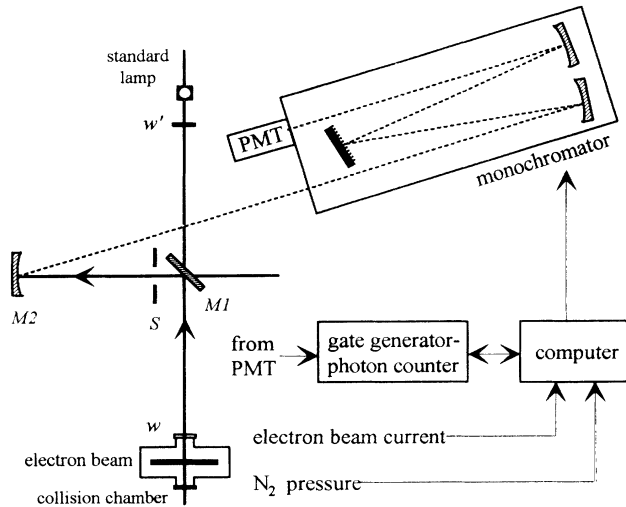
FIG. 2. Schematic diagram of the experimental apparatus. Mirror $M1$ rotates to accept emission from either the electron beam in the collision chamber or the standard lamp.

$D \rightarrow A(v',v'')$ emission band is obtained from the area under the PMT output versus wavelength curve of the band and Eq. (7) of Ref. [13]. For calibration, the plane mirror $M1$ is rotated 90° to receive emission from the standard lamp rather than the electron beam. For work in the uv, we use a deuterium lamp of known spectral irradiance as the standardization source. A window w' that is equivalent to the collision chamber window w ensures that the optical path of the emission from the calibration lamp is identical to that from the electron beam in the collision chamber.

Initially we employed an analog method to measure the PMT output during spectral scans. This arrangement used a mechanical chopper to modulate the electron-beam emission as it exited the collision chamber and a lock-in amplifier to receive the PMT output. The monochromator slowly scanned through the wavelength range of interest and the lock-in output was recorded on a strip chart. It became apparent that the extremely weak signal from the $D\,^2\Pi_g \rightarrow A\,^2\Pi_u$ emission required a more sensitive detection technique, so we turned to a digital photon-counting scheme.

In the photon-counting method, a modulating circuit chops the electron beam by varying the potential of the electron-gun control grid. Photon pulses from the PMT are collected by a photon counter that is turned on and off with two gates, A and B, of identical length τ. Gate A is open while the electron beam is on and contains the electron-beam emission plus any background sources of signal including PMT dark counts, cathode heater emission, and any other stray light. Gate B opens while the electron beam is off and it contains only the background signal. The $A - B$ signal contains only the signal due to electron-beam emission. A personal computer controls the monochromator, monitors the electron-beam current and N_2 pressure, and collects data from the photon counter. The computer steps the monochromator through the wavelength range in discrete intervals, and at each interval as many as 1×10^6 gate pairs are collected

by the photon counter. The computer records the data and advances the monochromator to the next interval and the process is repeated. To minimize the influence of systematic errors caused by drifting parameters during long runs, the entire wavelength range is scanned several times during the run. For calibration, the standard lamp with a mechanical chopper replaces the electron beam as the emission source. Gates of the same length τ are positioned within "on" and "off" portions of the mechanically chopped standard lamp signal. The great advantage the photon-counting method has over analog techniques is its signal-to-noise ratio. Because the monochromator can remain at each wavelength interval for long times, the signal-to-noise ratio can be greatly enhanced. This allows us to sacrifice signal strength by decreasing the monochromator slit widths in order to increase the spectral resolution, which is especially important for the present work as the $D \rightarrow A$ emission bands overlap significantly with numerous other nitrogen bands.

We find that the $D \rightarrow A$ emission signal is directly proportional to the N_2 gas pressure and to the electron-beam current for N_2 pressures below 10 mTorr and electron-beam currents below 350 μA used in this experiment. The polarization of the $D \rightarrow A$ emission has been measured at both 150 and 200 eV and found to be negligibly small. At lower energies, where the cross section is significantly smaller than at the 200-eV peak, the attenuation of the already weak emission from the $D \rightarrow A$ bands by the polarizer makes it difficult to accurately measure the polarization. The signal-to-noise ratio is very poor for our polarization measurement at 100 eV; nevertheless the data show no discernable polarization within the experimental uncertainty.

III. RESULTS

The $N_2^+\ D\,^2\Pi_g \rightarrow A\,^2\Pi_u$ emission bands occur in the wavelength range 2000–3100 Å. Our spectral scans of this wavelength region indicate that the $D \rightarrow A$ emission bands produced by electron impact on N_2 in the collision chamber are very weak, and most of these bands are masked or severely contaminated by other N_2 emission bands. For the above reasons we have measured the electron-impact optical cross sections of only the (7,8), (9,8), and (4,5) bands of the $D \rightarrow A$ emission.

The $D \rightarrow A$ (9,8) band overlaps somewhat with the $C\,^3\Pi_u \rightarrow B\,^3\Pi_g$ (4,1) band of N_2 in our scan of the emission signal versus wavelength. To correct for this overlap we extrapolate the scan curve of the $C \rightarrow B$ (4,1) band from a nonoverlapping region into the region where the two bands overlap so that we can isolate the portion of the emission signal due to the $C \rightarrow B$ (4,1) band alone. We estimate that this extrapolation correction procedure introduces an uncertainty of 12% to the measured cross section for the $D \rightarrow A$ (9,8) band at 200 eV. Likewise the $D \rightarrow A$ (7,8) band shows some overlap with the $c'_4\,^1\Sigma_u^+ \rightarrow a\,^1\Pi_g$ (1,2) band of N_2 and the same extrapolation method is used to separate the observed emission signal. The $D \rightarrow A$ (4,5) band is not appreciably contam-

inated by other N$_2$ bands, but its signal is considerably weaker than the (7,8) or (9,8) bands. We obtain the peak cross sections for the $D \rightarrow A$ (9,8), (7,8), and (4,5) bands as 2.5×10^{-21}, 3.0×10^{-21}, and 1.1×10^{-21} cm^2, respectively, and the corresponding uncertainties are 32%, 27%, and 31%.

We have measured the dependence of the $D \rightarrow A$ emission cross section on incident electron energy within the range of 75–1000 eV. Below 75 eV the $D \rightarrow A$ emission signal is too weak to allow us to clearly distinguish the $D \rightarrow A$ emission from the overlapping bands. In addition, the emission from the overlapping N$_2$ bands, the $C \rightarrow B$ and the $c_4' \rightarrow a$, increases significantly below 100 eV, further masking the $D \rightarrow A$ bands. The cross sections for the $D \rightarrow A$ (9,8), (7,8), and (4,5) bands show the same energy dependence. The values of the $D \rightarrow A$ emission cross section for these bands, relative to their respective peak values, are plotted as a function of electron energy in Fig. 3. The optical emission excitation function of the $D \rightarrow A$ system has a broad peak at about 200 eV. The cross-section data above 250 eV conform closely to an energy dependence of the form $E^{-1} \ln E$. We fit a smooth curve through all data points using a least-squares fit of the function [15],

$$Q(E) = \frac{1}{E E_{\text{ion}}} \left[A \ln \left[\frac{E}{E_{\text{ion}}} \right] + \sum_{i=1}^{N} B_i \left[1 - \frac{E_{\text{ion}}}{E} \right]^i \right],$$

(1)

where E_{ion} is the threshold energy of the N$_2^+(D\,^2\Pi_g)$ state relative to the N$_2(X\,^1\Sigma_g^+)$ state and A and B_i are adjustable parameters. Three terms in the sum are used for the curve in Fig. 3.

The $D\,^2\Pi_g$ state can radiatively decay to the $B\,^2\Sigma_u^+$ and $A\,^2\Pi_u$ states. We have found no experimental observation of the N$_2^+$ $D\,^2\Pi_g \rightarrow B\,^2\Sigma_u^+$ system in the literature. We have looked for the $D \rightarrow B$ emission in the spectral scans of the electron-beam emission in our experiment and found no discernable signal. If the emission intensity of the $D \rightarrow B$ bands can be neglected in comparison to the $D \rightarrow A$ bands, then it is possible to obtain the apparent excitation cross section of the vibrational level (v') of the N$_2^+$ $D\,^2\Pi_g$ electronic state by summing the optical emission cross sections for the $D \rightarrow A$ (v',v'') bands over all v''. Since we have measured the cross sections for the (4,5), (7,8), and (9,8) bands, we can obtain the cross sections for the $(4,v'')$, $(7,v'')$, and $(9,v'')$ bands with all values of v'' from the fact that the ratio of the optical emission cross sections of two transitions with the same upper level is equal to the ratio of the corresponding Einstein A coefficients. If we assume that the $D \rightarrow A$ electronic transition moment depends only weakly on the internuclear distance R, the Einstein A coefficient of a vibrational band of a given electronic transition is approximately proportional to the Franck-Condon factor $q(v' \rightarrow v'')$ and to the inverse third power of the wave-
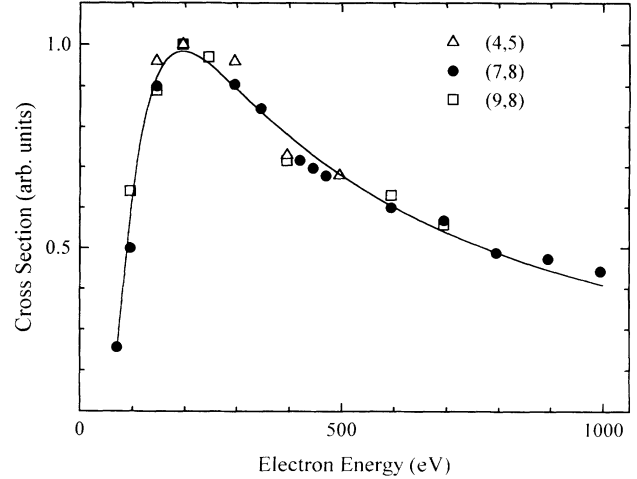
FIG. 3. Energy dependence for the emission cross sections of the (4,5), (7,8), and (9,8) $D \rightarrow A$ bands relative to their respective peak values. The solid curve is a least-squares fit of the function in Eq. (1).

length λ. Denoting the optical emission cross section for the $D \rightarrow A$ (v',v'') band as $Q(Dv' \rightarrow Av'')$, we have

$$\frac{Q(Dv' \rightarrow Av_i'')}{Q(Dv' \rightarrow Av_j'')} \approx \left[\frac{\lambda(Dv' \rightarrow Av_j'')}{\lambda(Dv' \rightarrow Av_i'')} \right]^3 \frac{q(Dv' \rightarrow Av_i'')}{q(Dv' \rightarrow Av_j'')}.$$

(2)

We have used the vibrational potential functions for the $D\,^2\Pi_g$ and $A\,^2\Pi_u$ states given in Ref. [10] to calculate the vibrational wave functions and the Franck-Condon factors. This allows us to determine the emission cross sections for each series of (v',v'') band with $v'=4$, 7, and 9. The apparent cross section for exciting the vibrational level v' of the N$_2^+$ $D\,^2\Pi_g$ state is given approximately by the sum of $Q(Dv' \rightarrow Av'')$ over v'' which is 4×10^{-20}, 5×10^{-20}, and 5×10^{-20} cm^2, respectively, for $v'=4$, 7, and 9 at 200 eV. We must emphasize that the above numbers should be regarded only as an estimate of the apparent cross section. For each v' level we have measured the cross section of only one (v',v'') band and therefore we are not able to test the accuracy of Eq. (2). Nevertheless these estimates allow us to make comparisons with the cross sections of the lower states of N$_2^+$ in the following section.

IV. DISCUSSION

In this section we discuss the production of the excited N$_2^+$ by electron impact in reference to the electronic structure of N$_2$ and N$_2^+$. The dominant electron configurations of the N$_2(X\,^1\Sigma_g^+)$ ground state, the N$_2^+(X\,^2\Sigma_g^+)$ ground state, and the first three excited states of N$_2^+$ are [10]

$N_2(X\,^1\Sigma_g^+)$: $(1\sigma_g)^2(1\sigma_u)^2(2\sigma_g)^2(2\sigma_u)^2(1\pi_u)^4(3\sigma_g)^2$,

$N_2^+(X\,^2\Sigma_g^+)$: $(1\sigma_g)^2(1\sigma_u)^2(2\sigma_g)^2(2\sigma_u)^2(1\pi_u)^4(3\sigma_g)$,

$N_2^+(A\,^2\Pi_u)$: $(1\sigma_g)^2(1\sigma_u)^2(2\sigma_g)^2(2\sigma_u)^2(1\pi_u)^3(3\sigma_g)^2$,

$N_2^+(B\,^2\Sigma_u^+)$: $\begin{cases}(1\sigma_g)^2(1\sigma_u)^2(2\sigma_g)^2(2\sigma_u)(1\pi_u)^4(3\sigma_g)^2 \\ (1\sigma_g)^2(1\sigma_u)^2(2\sigma_g)^2(2\sigma_u)^2(1\pi_u)^3(3\sigma_g)(1\pi_g)\end{cases}$,

$N_2^+(D\,^2\Pi_g)$: $\begin{cases}(1\sigma_g)^2(1\sigma_u)^2(2\sigma_g)^2(2\sigma_u)^2(1\pi_u)^2(3\sigma_g)^2(1\pi_g) \\ (1\sigma_g)^2(1\sigma_u)^2(2\sigma_g)^2(2\sigma_u)^2(1\pi_u)^4(1\pi_g)\end{cases}$.

For the $B\,^2\Sigma_u^+$ and $D\,^2\Pi_g$ states which show two entries, the upper configuration is the one that describes the respective state when the one-configuration approximation is used [16–18]. We will first analyze the cross-section data for the $X\,^2\Sigma_g^+$, $A\,^2\Pi_u$, and $B\,^2\Sigma_u^+$ states in the literature, and then compare them with the $N_2^+(D\,^2\Pi_g)$ data reported in the present work. This will be followed by a discussion of the relation to the experimental work on the $C\,^2\Sigma_u^+$ state [9].

Producing the ground-state N_2^+ ion $(X\,^2\Sigma_g^+)$ from the $N_2(X\,^1\Sigma_g^+)$ molecule entails the removal of an electron in the outermost $3\sigma_g$ orbital which is usually regarded as the major mechanism for producing N_2^+. Likewise, production of $N_2^+(A\,^2\Pi_u)$ and $N_2^+(B\,^2\Sigma_u^+)$ can be accomplished by removing, respectively, a $1\pi_u$ and a $2\sigma_u$ electron from $N_2(X\,^1\Sigma_g^+)$ and therefore is regarded as ionization of an inner valence electron. This is to be contrasted with the corresponding process for He, i.e., production of an excited $He^+(nl)$ ion from $He(1s^2)$, which is a two-electron process involving the simultaneous ionization of one electron and excitation of the other. Since the production of the N_2^+ in the $X\,^2\Sigma_g^+$ ground state and in the $A\,^2\Pi_u$ and $B\,^2\Sigma_u^+$ excited states involves the same kind of one-electron ionization process, we may expect a certain similarity in the cross-section data. We are not aware of any direct measurements of the electron-impact cross sections for $N_2^+(X\,^2\Sigma_g^+)$. However, cross sections have been reported [11,12] for the production of N_2^+ that include N_2^+ in the $X\,^2\Sigma_g^+$ ground state and in the excited electronic states. In Fig. 4 we plot the cross-section data for the $N_2^+(A\,^2\Pi_u)$ state, for the $N_2^+(B\,^2\Sigma_u^+)$ state, and for N_2^+ ions relative to their respective peak values versus the electron energy. All three curves are seen to be nearly identical. This indicates that the cross sections for production of $N_2^+(X\,^2\Sigma_g^+)$ have the same energy dependence as those of $N_2^+(A\,^2\Pi_u)$ and $N_2^+(B\,^2\Sigma_u^+)$. The energy dependences of the $N_2^+(B\,^2\Sigma_u^+)$ cross section reported in Refs. [1] and [4] differ somewhat from each other. We measured the $N_2^+(B\,^2\Sigma_u^+)$ cross sections up to 1000 eV and found the energy dependence very close to Ref. [4]. Thus we use the data of Ref. [4] in Fig. 4.

Stanton and St. John [1] measured optical emission cross sections for numerous bands of the N_2^+ $A\,^2\Pi_u \to X\,^2\Sigma_g^+$ system. By summing the cross sections over v'' for each v', they obtained peak apparent cross sections for the $N_2^+[A\,^2\Pi_u(v')]$ vibrational levels of 11×10^{-18}, 15×10^{-18} cm^2, 11.5×10^{-18}, 5.6×10^{-18},

2.7×10^{-18}, and 1.3×10^{-18} cm^2 for $v'=0$, 1, 2, 3, 4, and 5, respectively. Since the initial state of the electron-impact process is the ground vibrational level of the ground electronic state $(X\,^1\Sigma_g^+)$ of N_2, the direct cross sections for $N_2^+[A\,^2\Pi_u(v')]$ is approximately proportional to the Franck-Condon factors between $N_2[X\,^1\Sigma_g^+(v''=0)]$ and $N_2^+(A\,^2\Pi_u(v'))$. If we assume that the cascade contribution to the population of the $N_2^+[A\,^2\Pi_u(v')]$ level is small in comparison with direct excitation, we can compare the apparent cross sections with the Franck-Condon factors. Indeed the relative values of the $N_2^+[A\,^2\Pi_u(v')]$ cross sections cited above are 0.73:1.00:0.77:0.37:0.18:0.087, which agree well with the ratios of the corresponding Franck-Condon factors [6] of 0.85:1.00:0.67:0.35:0.15:0.062. For the $N_2^+[B\,^2\Sigma_u^+(v')]$ levels, Stanton and St. John [1] reported peak apparent cross sections of 22.3×10^{-18}, 2.6×10^{-18}, 0.21×10^{-18}, and 0.09×10^{-18} cm^2 for $v'=0$, 1, 2, and 3, respectively. Here the cross section decreases drastically with increasing v' in contrast to the $N_2^+[A\,^2\Pi_u(v')]$ cross sections. The reason for this is made apparent in Fig. 1 where we see a fairly close resemblance between the vibrational potential functions of the initial $[N_2(X\,^1\Sigma_g^+)]$ and final $[N_2^+(B\,^2\Sigma_u^+)]$ states of the electron-impact excitation process. For instance, the equilibrium distances for these two states are 1.098 and
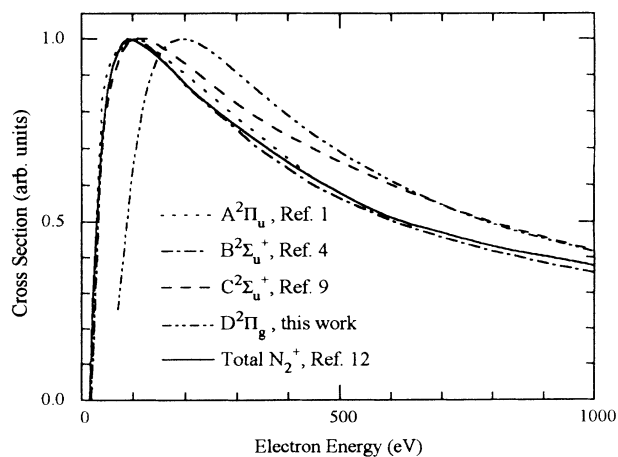
FIG. 4. Plots of the cross-section data vs electron energy for the $N_2^+(A\,^2\Pi_u)$, $N_2^+(B\,^2\Sigma_u^+)$, $N_2^+(C\,^2\Sigma_u^+)$, and $N_2^+(D\,^2\Pi_g)$ states, and for N_2^+ ions relative to their respective peak values.

1.078 Å, and the vibrational frequencies ω are 2359 and 2420 cm^{-1} [10]. As a result, the Franck-Condon factors between the $N_2[X\,^1\Sigma_g^+(v''=0)]$ and $N_2^+[B\,^2\Sigma_u^+(v')]$ levels tend toward a quasiorthogonal pattern, i.e., 0.886, 0.111, 0.002 34, and 0.000 014 2 (1.00:0.13:0.0026:0.000 016) for $v'=0$, 1, 2, and 3, respectively. The corresponding relative values of the $N_2^+[B\,^2\Sigma_u^+(v')]$ cross sections of Stanton and St. John [1] are 1.00:0.12:0.0094:0.0040. Again, the observed cross sections appear to track with the Franck-Condon factors, although the two sets of ratios agree only qualitatively for $v'=2$ and 3. The lack of quantitative agreement in the cases of $v'=2$ and 3 is not surprising because the very small Franck-Condon factors may be sensitive to uncertainties of the potential functions and because the apparent excitation cross sections may be strongly affected by cascade when the direct cross sections are very small.

The cross section for exciting the entire electronic state is obtained by summing all the cross sections for exciting the various vibrational levels associated with that electronic state. Using the data of Stanton and St. John [1] we obtain the cross section for producing the $A\,^2\Pi_u$ state by electron impact on N_2 as 4.8×10^{-17} cm^2 at 100 eV, and the corresponding cross section for $B\,^2\Sigma_u^+$ as 2.5×10^{-17} cm^2 at 100 eV. Itikawa et al. [12] gave the cross section for producing N_2^+ as 20×10^{-17} cm^2 at 100 eV. Based on the measurements of St. John and Stanton we obtain an estimate of the cross section for the $N_2^+(X\,^2\Sigma_g^+)$ ground state as 13×10^{-17} cm^2 at 100 eV. However, several conflicting sets of cross sections for the $N_2^+(A\,^2\Pi_u)$ state have appeared in the literature, and a discussion has been given by Piper et al. [8] who gave $(11.5\pm2.3)\times10^{-17}$ cm^2 as the cross section for $N_2^+(A\,^2\Pi_u)$ at 100 eV. If we adopt this value and combine it with the cross sections for producing N_2^+ ions and for $N_2^+(B\,^2\Sigma_u^+)$ cited earlier in this paragraph, we find the cross section for $N_2^+(X\,^2\Sigma_g^+)$ ranging from 8.3×10^{-17} to 3.7×10^{-17} cm^2. In view of the wide variance in the cross sections involved, we can only conclude that the cross sections for $N_2^+(X\,^2\Sigma_g^+)$ and $N_2^+(A\,^2\Pi_u)$ are roughly comparable, but the $N_2^+(B\,^2\Sigma_u^+)$ cross sections are probably several times smaller. This trend is consistent with the similar one-electron mechanism for exciting the three lowest electronic states.

Let us turn our attention to the $N_2^+(D\,^2\Pi_g)$ state. The excitation function shown in Fig. 3 is replotted in Fig. 4. Here we see that the energy dependence of the $N_2^+(D\,^2\Pi_g)$ cross sections is quite distinct from the curves for the $X\,^2\Sigma_g^+$, $A\,^2\Pi_u$, and $B\,^2\Sigma_u^+$ states. In particular, the maximum cross section for $N_2^+(D\,^2\Pi_g)$ occurs at 200 eV as opposed to 100 eV for the other three states. Inspection of the dominant electron configurations shows that the $D\,^2\Pi_g$ state differs from the $X\,^2\Sigma_g^+$, $A\,^2\Pi_u$, and $B\,^2\Sigma_u^+$ states in that one cannot produce $N_2^+(D\,^2\Pi_g)$ by simply removing one electron from $N_2(X\,^1\Sigma_g^+)$. Converting $N_2(X\,^1\Sigma_g^+)$ into the $(1\sigma_g)^2(1\sigma_u)^2(2\sigma_g)^2(2\sigma_u)^2(1\pi_u)^2(3\sigma_g)^2(1\pi_g)$ configuration of $N_2^+(D\,^2\Pi_g)$ entails the simultaneous removal of a $1\pi_u$ electron and excitation of an electron from the $1\pi_u$

orbital to $1\pi_g$. Likewise, production of the other dominant configuration of $N_2^+(D\,^2\Pi_g)$, $(1\sigma_g)^2(1\sigma_u)^2(2\sigma_g)^2(2\sigma_u)^2(1\pi_u)^4(1\pi_g)$, from $N_2(X\,^1\Sigma_g^+)$ involves the removal of a $3\sigma_g$ electron in addition to the $3\sigma_g\to1\pi_g$ excitation. These processes involve two active electrons in contrast to the one-electron ionization process for the production of $N_2^+(X\,^2\Sigma_g^+)$, $N_2^+(A\,^2\Pi_u)$, and $N_2^+(B\,^2\Sigma_u^+)$. The difference between those two kinds of processes is probably related to the observed difference in the shape of the excitation function between the $D\,^2\Pi_g$ state and the three lower electronic states of N_2^+. Further studies should be valuable.

Another feature that distinguishes the $D\,^2\Pi_g$ state from the $X\,^2\Sigma_g^+$, $A\,^2\Pi_u$, and $B\,^2\Sigma_u^+$ states is that the classical turning points for all vibrational levels of the $D\,^2\Pi_g$ state up to $v=9$ are well outside the classically allowed region of the ground vibrational wave function of the $N_2(X\,^1\Sigma_g^+)$ electronic state as illustrated in Fig. 1. This feature makes the production of $N_2^+(D\,^2\Pi_g)$ unfavorable in comparison with the N_2^+ ions in the three lower electronic states, and is reflected in the observed cross sections for $D\,^2\Pi_g$ being orders of magnitude smaller than those for the $X\,^2\Sigma_g^+$, $A\,^2\Pi_u$, and $B\,^2\Sigma_u^+$ states.

Above the $D\,^2\Pi_g$ state of N_2^+ is the $C\,^2\Sigma_u^+$ state. Excitation of the $C\,^2\Sigma_u^+$ state by electron impact on N_2 has been studied by van de Runstraat, de Heer, and Grovers [9]. The $C\,^2\Sigma_u^+$ state is described primarily by the electron configuration $(1\sigma_g)^2(1\sigma_u)^2(2\sigma_g)^2(2\sigma_u)^2(1\pi_u)^3(3\sigma_g)(1\pi_g)$ but configuration interaction introduces an admixture of the major configuration of the $B\,^2\Sigma_u^+$ state, i.e., $(1\sigma_g)^2(1\sigma_u)^2(2\sigma_g)^2(2\sigma_u)(1\pi_u)^4(3\sigma_g)^2$ [17,19]. The latter configuration is related to the $N_2(X\,^1\Sigma_g^+)$ state by removal of one electron $(2\sigma_u)$ as explained earlier, whereas a two-electron process is involved in generating the former configuration from $N_2(X\,^1\Sigma_g^+)$. Thus two mechanisms are available for production of $N_2^+(C\,^2\Sigma_u^+)$, i.e., the one-electron ionization of $2\sigma_u$ and the two-electron process of $(1\pi_u)^4(3\sigma_g)^2\to(1\pi_u)^3(3\sigma_g)(1\pi_g)$. Since the one-electron mechanism is connected to the minor configuration of the $C\,^2\Sigma_u^+$ state, its importance depends on the weighting of the minor configuration on the $C\,^2\Sigma_u^+$ state and the relative efficiency of the two-electron process versus the one-electron ionization. If the excitation of $N_2^+(C\,^2\Sigma_u^+)$ is mostly due to the one-electron mechanism, we would expect similar excitation behavior for the $B\,^2\Sigma_u^+$ and $C\,^2\Sigma_u^+$ states with their relative cross sections dictated mainly by the weighting of the $(1\sigma_g)^2(1\sigma_u)^2(2\sigma_g)^2(2\sigma_u)(1\pi_u)^4(3\sigma_g)^2$ configuration in the wave functions. In Ref. [9] it is assumed that the two-electron mechanism can be neglected in comparison with one-electron mechanism in the production of $N_2^+(C\,^2\Sigma_u^+)$; this assumption was adopted to analyze the optical data of the $C\,^2\Sigma_u^+\to X\,^2\Sigma_g^+$ emission bands produced by electron excitation. Determination of the $C\,^2\Sigma_u^+$ cross section was complicated by the possibility of predissociation for the vibrational levels of $C\,^2\Sigma_u^+$ above $v=3$ and by the fact that the measurement of absolute cross section and its energy dependence was made from

the combined optical signal of the (1,7), (2,8), (0,6), and (3,9) bands of the (v',v'') vibrational members. Nevertheless the results of the cross section for $C\,^2\Sigma_u^+$ are consistent with the assumption of the one-electron mechanism being the major contributor. In Fig. 4 we plot the energy dependence of the cross section for emission from the $C\,^2\Sigma_u^+$ state ("combined" bands) as reported in Ref. [9]. Interestingly, this curve follows those of the $A\,^2\Pi_u$ and $B\,^2\Sigma_u^+$ closely up to 100 eV, and moves toward the $D\,^2\Pi_g$ curve at higher energies, finally merging with the $D\,^2\Pi_g$ curve above 700 eV. It is possible that this crossing behavior suggests the transition from the one-electron process into an energy regime where the two-electron mechanism becomes more significant. Electron excitation experiments for the $C\,^2\Sigma_u^+$ state are difficult because the $C\,^2\Sigma_u^+ \to X\,^2\Sigma_g^+$ emission bands are in the range of 2230–1270 Å and the bands with the same Δv are very close together. However, a comprehensive study of the excitation of the $N_2^+(C\,^2\Sigma_u^+ \to X\,^2\Sigma_g^+)$ emission bands by electron impact on N_2 should be important in understanding the excitation mechanism.

V. SUMMARY AND CONCLUSIONS

We have measured the optical emission cross sections for three vibrational bands of the $N_2^+(D\,^2\Pi_g \to A\,^2\Pi_u)$ electronic transition resulted from electron impact on N_2. From the optical data we obtain estimates for the cross sections for the production of $N_2^+(D\,^2\Pi_g)$ with $v = 4, 7,$ and 9 as 4×10^{-20}, 5×10^{-20}, and 5×10^{-20} cm^2, respectively, at 200 eV. The excitation function has also been measured. By combining these data with the known cross sections and excitation functions of $N_2^+(A\,^2\Pi_u)$ and $N_2^+(B\,^2\Sigma_u^+)$ and with the ionization cross sections for producing N_2^+, we study the systematics of the cross sections for producing N_2^+ ions in various electronic states. The $X\,^2\Sigma_g^+$ ground state of N_2^+ and the $A\,^2\Pi_u$ and $B\,^2\Sigma_u^+$ excited states are alike in that they can be generated from $N_2(X\,^1\Sigma_g^+)$ by removal of one electron in

the $3\sigma_g$, $1\pi_u$, and $2\sigma_u$ orbitals, respectively. The shapes of the excitation functions for these three electronic states are found to be virtually identical. The $N_2^+(X\,^2\Sigma_g^+)$ and $N_2^+(A\,^2\Pi_u)$ cross sections are of roughly comparable magnitude and are probably several times larger than the $N_2^+(B\,^2\Sigma_u^+)$ cross sections, consistent with the one-electron-removal mechanism for all three states. The relative cross sections for the various vibrational levels of the $A\,^2\Pi_u$ and $B\,^2\Sigma_u^+$ conform to their corresponding Franck-Condon factors with respect to the ground vibrational level of the $X\,^1\Sigma_g^+$ ground electronic state of N_2.

The excitation data for the $D\,^2\Pi_g$ state appear to be quite different. Production of the $N_2^+(D\,^2\Pi_g)$ ion from the $N_2(X\,^1\Sigma_g^+)$ molecule entails two active electrons instead of removal of just one electron as described in the preceding paragraph. The energy dependence of the cross section for excitation of the $D\,^2\Pi_g$ state is different from that of the $X\,^2\Sigma_g^+$, $A\,^2\Pi_u$, and $B\,^2\Sigma_u^+$ states. Moreover the $D\,^2\Pi_g$ cross sections are orders of magnitude smaller than those of the three lower electronic states.

It is interesting to consider for comparison the formation of excited atomic ions by electron impact on the ground-state neutral atoms. The classical case is the production of He$^+(nl)$ from He($1s^2$) which involves two active electrons and is known appropriately as simultaneous ionization and excitation. The peak cross section for He$^+(2p)$ is 6×10^{-19} cm^2 [20]. The same two-electron mechanism is also responsible for turning Ne($2p^6$) into Ne$^+(2p^4nl)$. Typical peak cross sections for the $3p \to 3s$ emission are in the range of 10^{-19} to 10^{-20} cm^2 [21]. These cross sections are much smaller than those of $N_2^+(A\,^2\Pi_u)$ and $N_2^+(B\,^2\Sigma_u^+)$, because Ne$^+(2p^4nl)$ cannot be generated from Ne($2s^22p^6$) by a one-electron process.

[1] P. N. Stanton and R. M. St. John, J. Opt. Soc. Am. **59**, 252 (1969).
[2] J. W. McConkey, J. M. Woolsey, and D. J. Burns, Planet. Space Sci. **15**, 1332 (1967).
[3] B. N. Srivistava and I. M. Mirza, Phys. Rev. **168**, 86 (1968).
[4] W. L. Borst and E. C. Zipf, Phys. Rev. A **1**, 834 (1970).
[5] F. R. Simpson and J. W. McConkey, Planet. Space Sci. **17**, 1941 (1969).
[6] B. N. Srivistava and I. M. Mizra, Can. J. Phys. **47**, 475 (1969).
[7] R. F. Holland and W. B. Maier II, J. Chem. Phys. **56**, 5229 (1972); **58**, 2672 (1973).
[8] L. G. Piper, B. D. Green, W. A. M. Blumberg, and S. J. Wolnik, J. Phys. B **19**, 3327 (1986), and references therein.
[9] C. A. van de Runstraat, F. J. de Heer, and T. R. Grovers, Chem. Phys. **3**, 431 (1974).
[10] A. Loftus and P. H. Krupenie, J. Phys. Chem. Ref. Data **6**, 113 (1977).
[11] P. B. Armentrout, S. M. Tarr, A. Dori, and R. S. Freund,

J. Chem. Phys. **75**, 2768 (1986).
[12] Y. Itakawa, M. Hayashi, A. Ichimura, K. Omda, K. Sakimoto, K. Takayanagi, M. Nakamura, and T. Takayanagi, J. Phys. Chem. Ref. Data **15**, 985 (1986).
[13] A. R. Filippelli, S. Chung, and C. C. Lin, Phys. Rev. A **29**, 1709 (1984).
[14] J. S. Allen and C. C. Lin, Phys. Rev. A **39**, 383 (1989).
[15] K. L. Bell, H. B. Gilbody, J. G. Hughes, A. E. Kingston, and F. J. Smith, J. Phys. Chem. Ref. Data **12**, 891 (1983).
[16] P. E. Cade, K. D. Sales, and A. C. Wall, J. Chem. Phys. **44**, 1973 (1966).
[17] R. S. Mulliken, in *The Threshold of Space*, edited by M. Zelikoff (Pergamon, New York, 1957), p. 169.
[18] F. Guérin, Theor. Chim. Acta **17**, 97 (1970).
[19] J. C. Lorquet and M. Desouter, Chem. Phys. Lett. **16**, 136 (1972).
[20] J. L. Forand, K. Becker, and J. W. McConkey, J. Phys. B **18**, 1409 (1985).
[21] K. G. Walker and R. M. St. John, Phys. Rev. A **6**, 240 (1972).